Tsunami Efficiency due to Very Slow Earthquakes

Sebastian Riquelme[1] and Mauricio Fuentes[2]

[1]University of Chile
[2]Department of Geophysics

November 26, 2022

Abstract

Often, tsunamis have been treated as a static problem. First studies demonstrated that for earthquake rupture velocities in the span of 1.5 km/s to 3 km/s, the kinematic and static part of the tsunami can be treated separately. The deformation generated by an earthquake is copied into the sea surface and then the tsunami is propagated. However, very slow earthquake rupture velocities in the span of 0.1 to 1 km/s have not been included into tsunami modeling. Here, we calculate tsunami efficiency, based on Kajiura's definition, for different models. We demonstrate that rupture velocity cannot be neglected for very slow events, i.e, rupture velocities slower than 0.5 km/s. We calculate a relation between Magnitude, Rupture Velocity and Tsunami Amplitude to the Efficiency of very slow tsunamigenic earthquakes. Megathrust earthquakes (Mw >8.5) with very slow rupture velocity amplify energy from 10 to 60 times larger than moderate to large earthquakes.

Tsunami Efficiency due to Very Slow Earthquakes

S. Riquelme[1] and M. Fuentes[2]

[1]National Seismological Center, University of Chile, Santiago, Chile

[2]Programa de Riesgo Sísmico, University of Chile, Santiago, Chile

Corresponding author: Sebastian Riquelme (sebastian@dgf.uchile.cl)

Key Points:

- We Studied the Tsunami Efficieny due to very slow earthquakes.
- Amplification of efficiency depends on directivty and rupture velocity.
- We calculated a relationship of Tsunami Efficieny as function of Rupture Velocity, Tsunami Velocity and Moment Magnitude.

Abstract

Often, tsunamis have been treated as a static problem. First studies demonstrated that for earthquake rupture velocities in the span of 1.5 km/s to 3 km/s, the kinematic and static part of the tsunami can be treated separately. The deformation generated by an earthquake is copied into the sea surface and then the tsunami is propagated. However, very slow earthquake rupture velocities in the span of 0.1 to 1 km/s have not been included into tsunami modeling. Here, we calculate tsunami efficiency, based on Kajiura's definition, for different models. We demonstrate that rupture velocity cannot be neglected for very slow events, i.e, rupture velocities slower than 0.5 km/s. We calculate a relation between Magnitude, Rupture Velocity and Tsunami Amplitude to the Efficiency of very slow tsunamigenic earthquakes. Megathrust earthquakes (Mw >8.5) with very slow rupture velocity amplify energy from 10 to 60 times larger than moderate to large earthquakes.

1 Introduction

The way tsunamis transfer energy into the ocean has been studied by several authors (Ward 1980, Tang et al. 2012, Dutykh and Dias 2009, Titov et. al 2016) . Most of the time, the kinematic part is not considered into tsunami modeling. This was first proposed by Kajiura (1970). Kajiura studied this by separating the dynamic and the static part. He found out that if the rupture velocity is larger than the tsunami velocity, the kinematic effect of the rupture can be neglected and the tsunami is not affected by the temporal properties of the source.

Tsunami Earthquakes (Kanamori, 1970) are tsunamigenic earthquakes that release energy in a very low frequency content. These are events that present ruptures that propagate slower than regular tsunamigenic earthquakes, produce less shaking than expected and small seismic wave amplitudes. They do not generate large amplitude seismic waves, therefore, most of them are not felt by the population, and do not produce structural damage. The understanding of these types of earthquakes is still in debate, however, there are many hypotheses that explain their nature such as, rheological properties, horizontal coseismic contributions, non-linear effects of the crust deformation, slow velocity rupture, among others.

In 1992, the first tsunami earthquake ever recorded by broadband seismometers occurred and it was possible to infer source properties such as: seismic moment, rupture velocity, shear modulus, stress drop and main slip location (Kanamori, 1993; Satake, 1994; Geist, 2001; Kikuchi and Kanamori, 1993). Kanamori (1993), proposed a rupture propagating in a sediments-filled medium which would lead to a slow rupture velocity and it would also explain the rheological properties change.

Ma (2012) explained that it is possible to generate tsunamis from slow earthquakes changing the pore pressure as the earthquake occurs. In his work, simulations of dynamic pore pressure changes show that when the dynamic pore pressure increases, due to up-dip rupture propagation leads to widespread yielding within the wedge; increasing the seafloor displacement. Ma and Hirakawa (2013), also suggest that due to dynamic wedge failure, it is possible to generate scenarios with more deformation at the trench, a slow rupture velocity and less seismic moment in the fault plane.

The 1947 Earthquake in New Zealand is another evidence of very slow earthquakes. Bell et. al. (2014) identified two tsunami earthquakes in New Zealand, the 1947 Offshore Poverty Bay and the Tolaga Bay events. The rupture velocity for these earthquakes was estimated between 0.15 to 0.30 km/s. This work argues that the slow-rupture would be responsible for the large run-up heights (relative to the magnitude) for both events. The maximum observed run-ups for the Offshore Poverty Bay and for the Tolaga Bay events are 10 and 6 m respectively. A very large coda and very small amplitude are necessary to model local seismograms that recorded the events, that are explained by very slow rupture velocities (< 1 km/s).

Todorovska and Trifunac (2001) studied the initial amplitude variation when the rupture velocity is included in a uniform source. They found that there exists a directivity wave focusing due to seafloor uplift oscillations coming faster behind other slowly developing waves when a tsunami propagates. The maximum amplification value occurs when the tsunami propagation velocity equals the earthquake rupture velocity. The uplifted segments travel at the same velocity as the uplifted water, and as the process evolves, the tsunami amplitude progressively increases due to constructive interference of the initial and subsequent waves created.

Fuentes et al. (2018) studied the tsunami run-up behavior, considering variations on temporal source parameters such as rise time and rupture velocity through the construction of a (1+1)-D analytical model. They found that rupture velocities of the order of 0.1-0.5 km/s show run-up amplifications up to 5 times compared with the static case. Williamson et al. (2019) studied the relationship between rupture kinematic properties and tsunami evolution. They found that earthquake rupture velocity variations down to 1.5 km/s had a small effect on tsunami propagation.

Since it is known that very slow earthquake rupture can increase tsunami amplitudes and the run-up (Riquelme et. al. 2020 and Fuentes et. al 2020). We calculate tsunami energy efficiency when earthquakes present very slow earthquake rupture velocity, as a function of moment magnitude, earthquake rupture and tsunami velocities. We also explain by theoretical arguments the tsunami energy efficiency-behaviour under very-slow earthquake-rupture velocities.

2 Methodology

Miyoshi (1954) defined the tsunami efficiency as

$$f = \frac{E_D}{E_S}$$

where E_D is the dynamic energy

$E_D = \rho g \int_0^T \int_S \zeta_t(x,y,t)\eta(x,y,t)dxdydt$ $\zeta_t(x,y,t)$ is the seafloor deformation and $\eta(x,y,t)$ is the wave amplitude.

$$E_S = \rho g \int_0^T \int_S \zeta_t(x,y,t)[h(x,y) - \zeta(x,y,t)]\,dxdydt$$

where S is the source area, T the source duration, ρ is the water density and g the gravity acceleration. Kajiura (1970) studied a different efficiency-like ratio as $\frac{E_D}{E_{D_0}}$.

E_{D_0} is the same dynamic energy for an analytical reference model (figure 1). In this study, we will take the corresponding value when rupture velocity is infinite.

In Kajiura (1970) model, T is the rise time, since there is no rupture velocity included. To extend this definition, we employ the analytical solution of amplitude $\eta(x,y,t)$ as function of V_r and $c_0 =: \sqrt{gh}$ obtained from Fuentes et al. (2020) to include the effect of the rupture. In the general case of a bilateral rupture composed by two segments L_1 and L_2, T is taken as the duration of the rupture process: $T = \frac{max(L_1,L_2)}{V_r} + t_R$, where V_r is the rupture velocity and t_R the rise time. Note that when V_r tend to infinity, one retrieves the same Kajiura's formula. Other observation is that depending on the wave pattern of the initial condition, E_D does admit negative values.

Then, we numerically compute the tsunami efficiency associated with a uniform wave amplitude for two different types of ruptures: Unilateral and Bilateral. For these ruptures, we calculate the dynamic and static energy as defined by Kajiura for Vr = 0.1, 0.2, 0.3, 0.4, 0.5, 0.6, 0.7, 0.8 , 0.9, 1, 1.5 and 2 km/s, using magnitudes of 6.0, 6.5, 7.0, 7.5, 8, 8.5, 9, 9.5 and different depths 2,4,6 ,8, 10 km emulating bathymetric depths around the globe.

We use the scaling law of Blaser et al. (2010) to associate a magnitude with the fault size and thus, to calculate dynamic and static energy for each model.

We also perform a few tests without causality (or no directivity) to show that the classical tsunami approximation in terms of maximum run-up height tends to the static case. These tests are key to prove that the amplification not just depends on the slowness of the source, but the earthquake directivity plays a key role on the amplification. We model the run-up because this is a static parameter which depends on the source; size, spatial and temporal complexity, directivity, bathymetry; and its maximum value is only referred to a spatial point R (x,y) and the end of the tsunami propagation, therefore at the ends of the tsunami process the run-up it is allow us to infer the energy distribution.

3 Results

Here, we show the results for a 4 km depth ocean (c=0.198 km/s). Full results are in the supplementary material for 6, 8, 10 km depth. We calculated the ratio $\frac{E_D}{E_{D_0}}$ defined by the extended definition of efficiency formula (Table 1 and Table 2).

The tsunami velocity c_0 in a 4 km depth bathymetry is 0.198 km/s. The maximum augmentation is observed when the earthquake rupture velocity is close to the tsunami velocity. This effect, of course, increases as the magnitude increases.

We observe a larger augmentation in the case of the unilateral rupture. This is because the rupture is longer, therefore, the tsunami has more time to amplify its energy until it reaches the edges of the fault (Fuentes et. al. 2020). The starting point splits the coupling energy according to how much earthquake area is available to break. Same results apply for the cases of 6, 8, and 10 km depth (see supplementary material).

For a Mw 9.5 earthquake, the effect of the magnitude predominates over the type of rupture. However, for both cases the augmentation is larger when $V_r = c_0$.

To verify that directivity, it is necessary to explain the mechanism behind the physics of very slow-rupture tsunamis. We create 20 heterogenous (Andrews 1980, 1981) earthquake sources without directivity. We generate a source with rupture starting points, i.e different hypocenters, each one of them has a rupture velocity of 0.2 km/ s in a 4 km depth ocean. The hypocenters are distributed along the rupture area with no causality, in this way we partially eliminate the effect of directivity. Obviously, as many starting rupture points we include, hypothetically, directivity would be totally eliminated when infinite of these “hypocenters” are acting together.

We perform these tests in a simple bathymetry including 20 heterogeneous sources. To eliminate the effect of directivity we model a group of 5 scenarios with 12, 24, 48, 72 and 100 “hypocenters”; setting a simple bathymetry of a 4 km ocean depth and 222 km from the trench to the coast with an inclination of 1.032° (figure S1) . These hypocenters are randomly located in the source.

Tsunami simulations were modeled with non-linear Boussinesq equations in order to take into account dispersive effects, by using the tsunami simulation code JAGURS (Baba et al. 2017), which also allows to onsider effects of elastic deformation of the seafloor caused by the weight of the water column, variations in the seawater density along a vertical profile.

The temporal evolution of the source is constructed as follows: 1. The inclusion of a temporal description of the slip distribution, i.e, the kinematic rupture process. 2. Using Okada’s equation (Okada, 1985) and horizontal contributions (Tanioka and Satake (1996)) to calculate the seafloor deformation for each time step. Therefore, at every time step, the static deformation is transferred to the sea surface respecting the points inside the rupture front activation, mimicking an active tsunami generation

The results show that the run-up in these cases tends to become similar to the heterogeneous static case . This occurs because the scenarios do not have enough area to develop directivity, when we add hypocenters to the source, the effect of directivity becomes lower and tends to the static case.

4 Discussion and Conclusions

A plausible way to produce large tsunamis near the trench would be with a change in the pore pressure. This would increase the deformation (Ma, 2012). Ma and Nie (2019) showed that an inelastic rupture for the Tohoku 2011 event would augment the deformation, then the slip values found by several authors would not be necessary to produce such a large deformation on the seafloor. The 1896 Sanriku earthquake also presents some features that might think this earthquake was caused by additional deformation in the prism (Tanioka and Seno 2001) .In this case, is not necessary to add more slip at the source, but with more displaced material in the trench it was observed that in three mareographs Hanasaki, Choshi and Ayukawa, fitted accurately their amplitude with the synthetics mareographs created from additional deformation. This earthquake would be another example of slow rupture due to inelasticity.

Inelastic deformation can cause slow rupture velocity because it is an energy sink. This would be distributed as heat which would be related to the low frequency content of the slow component in tsunamigenic earthquakes. The reduction of rupture velocity depends on how strong the inelastic deformation is. In the northern part of the 2004 Sumatra earthquake, there could have been a lot of inelastic deformation due to the presence of rich sediments, which may explain the intriguing observations. At the Bengal Bay, the intensities were very low (III-IV) but the tsunami was large (Lay et al. 2005). Another explanation of such slow rupture for this event would be the 90º E ridge, this would be a structural barrier that may result in slow rupture (Gahalut et. al., 2010).

It has been observed in the Tohoku 2011 earthquake and the Illapel earthquakes a slow rupture behavior towards the trench, the rupture velocity for the first case was slow as 1.5 km/s (Lay et al 2011) and for the second one 1.8 km/s.

The pore pressure can change dynamically during earthquake rupture if there is a change in mean normal stress. So, in subduction zones, up-dip rupture propagation can increase pore pressure significantly in the overriding wedge leading to a larger deformation not necessarily with more slip in the rupture.

An evidence of inelastic slow rupture is the Kaikoura earthquake in its Papatea fault segment (Diederichs et. al., 2019). Back projection models do not reconcile the observations obtained in the field and differential lidar. It seems that there exists a slow component not observed by this technique. Therefore an open discussion arises: what zones in the world due to rheological properties are prone to have slow rupture velocities?. Sedimentary wedges with low shear modulus are potentially the ones that can present an inelastic slow rupture, however this is still in debate. Under unique conditions, the ocean depth (h) would produce the tsunami velocity c_0 which would couple with rupture velocity , this would increase the tsunami and run-up amplitudes.

As it was proven by Riquelme et al. (2020) and Fuentes et al. (2020), the tsunami amplitudes augment when the rupture velocity combined with the directivity effect are acting together. Also the largest effect is found when the rupture velocity is equal to the tsunami velocity. The efficiency $\frac{E_D}{E_{D_0}}$ augments when very slow rupture are included. In the classical tsunami formulation, the rupture velocity was not taken into account because earthquakes were meant to be fast enough to avoid it. However the scenarios with random hypocenters explain that both effects are necessary to increase the run-up in these cases.

We have proven that the effect of amplitude augmentation is related to directivity and not just to deformation, the heterogeneous sources with no causality in the rupture show that without directivity but the same deformation of a Mw 9.0 earthquake will not increase the tsunami amplitude. The results are that for an earthquake with no directivity there is no augmentation either in the amplitude or the run-up. In fact, this scenario is equivalent to the static case.

The ratio between dynamic energy (E_D) and dynamic energy with infinite rupture velocity (E_{D_0}) explains how large the amplification is due to slow rupture velocity. When the rupture velocity is between 0.2 to 0.3 km/s associated to any magnitude, the amplitude amplification appears, the maximum amplification occurs as expected when the earthquake rupture velocity is equal to the tsunami velocity.

The ocean and the earth are weakly coupled due to the low water compressibility value, then it is still necessary to have large earthquakes to produce tsunamis. Therefore, magnitude is a proxy of the size of the tsunami, slip distribution a proxy of how large the amplitude and run-up would be in specific places in the near field; and directivity and rupture velocity are a measure of how large amplification is expected towards one direction or another. Then, large tsunamigenic earthquakes tend to produce larger amplitude amplification when they are slower, and small earthquakes do not amplify as much as the large ones do, but they still amplify. This would be an example of slower earthquakes getting larger amplifications than smaller ones (Figure 3) . Recall, energy is proportional to the square of the wave amplitudes, amplification process is controlled by other physical processes, which leads to, theoretically, extreme tsunami efficiency, as Figure 3 shows, in a hypothetical very slow Mw 9.5 earthquake.

The amplification follows the tsunami physics, it is necessary to have large earthquakes (Mw > 7.5) to produce tsunamis. Small earthquakes, even with slow velocity rupture and directivity effects, are not capable of producing large tsunamis. There is no coupling between tsunami velocity and earthquake rupture velocity when there is no directivity from the earthquake rupture, then this feature occurs only when slow rupture and directivity are present.

Acknowledgments, Samples, and Data

We thank Patricio Toledo who made suggestions to improve the manuscript. We thank Sebastian Arriola who performed the tsunami acausal simulations . This work was partially supported by Programa de Riesgo Sismico of the University of Chile.. Data of maximum tsunami amplitudes and run-up series and Data of Tsunami Efficiency versus ratio of tsunami and earthquake rupture velocity are available at supplementary material and in the following link https://zenodo.org/record/3829100#.Xr7Gh2hKg2x

References

Andrews, D. J. (1980). A stochastic fault model: 1. Static case. Journal of Geophysical Research: Solid Earth, 85(B7), 3867-3877

Andrews, D. J. (1981). A stochastic fault model: 2. Time-dependent case. Journal of Geophysical Research: Solid Earth, 86(B11), 10821-10834.

Baba, T., Allgeyer, S., Hossen, J., Cummins, P. R., Tsushima, H., Imai, K., ... & Kato, T. (2017). Accurate numerical simulation of the far-field tsunami caused by the 2011 Tohoku earthquake, including the effects of Boussinesq dispersion, seawater density stratification, elastic loading, and gravitational potential change. Ocean Modelling, 111, 46-54.

Bell, R., Holden, C., Power, W., Wang, X., & Downes, G. (2014). Hikurangi margin tsunami earthquake generated by slow seismic rupture over a subducted seamount. Earth and Planetary Science Letters, 397, 1-9

Dutykh, D., & Dias, F. (2009). Energy of tsunami waves generated by bottom motion. Proceedings of the Royal Society A: Mathematical, Physical and Engineering Sciences, 465(2103), 725-744.

Fuentes, M., Riquelme, S., Ruiz, J., & Campos, J. (2018). Implications on 1+1 D Tsunami runup modeling due to time features of the earthquake source. Pure and Applied Geophysics, 175(4), 1393-1404.

Fuentes, M., Uribe F., Riquelme, S., & Campos, J.Analytical Model for Tsunami Propagation including Source Kinematics. https://presentations.copernicus.org/EGU2020/EGU2020-1956_presentation.pdf. EGU 2020.

Fujii, Y., & Satake, K. (2007). Tsunami source of the 2004 Sumatra–Andaman earthquake inferred from tide gauge and satellite data. Bulletin of the Seismological Society of America, 97(1A), S192-S207.

Gahalaut, V. K., Subrahmanyam, C., Kundu, B., Catherine, J. K., & Ambikapathy, A. (2010). Slow rupture in Andaman during 2004 Sumatra–Andaman earthquake: a probable consequence of subduction of 90 E ridge. Geophysical Journal International, 180(3), 1181-1186.

Geist, E. L., & Bilek, S. L. (2001). Effect of depth-dependent shear modulus on tsunami generation along subduction zones. Geophysical research letters, 28(7), 1315-1318.

Hammack, J. L. (1973). A note on tsunamis: their generation and propagation in an ocean of uniform depth. Journal of Fluid Mechanics, 60(4), 769-799.

Kajiura K., 1970. Tsunami source, energy and the directivity of wave radiation, Bull. Earthq. Res. Institute. 48, 835–869.

Kanamori, H. (1972). Mechanism of tsunami earthquakes. Physics of the earth and planetary interiors, 6(5), 346-359.

Kanamori, H., and M. Kikuchi (1993), The 1992 Nicaragua earthquake: A slow tsunami earthquake associated with subducted sediments, Nature, 361(6414), 714–716, https://doi.org/10.1038/361714a0.

Lay, T., Kanamori, H., Ammon, C. J., Nettles, M., Ward, S. N., Aster, R. C., ... & DeShon, H. R. (2005). The great Sumatra-Andaman earthquake of 26 december 2004. Science, 308(5725), 1127-1133.

Ma, S., and E. T. Hirakawa (2013), Dynamic wedge failure reveals anomalous energy radiation of shallow subduction earthquakes, Earth Planet. Sci. Lett., 375, 113 - 122, doi: 10.1016/j.epsl.2013.05.016.

Ma, S., & Nie, S. (2019). Dynamic wedge failure and along-arc variations of tsunamigenesis in the Japan Trench margin. Geophysical Research Letters, 46. https://doi.org/10.1029/2019GL083148.

Ma, S. (2012), A self-consistent mechanism for slow dynamic deformation and tsunami generation for earthquakes in the shallow subduction zone, Geophys. Res. Lett., 39, L11310, doi:10.1029/2012GL051854.

Miyoshi H., Efficiency of the Tsunami Journal of the Oceanographical Society of Japan, Vol. 10 (No. 1), pp. 11-14, 1954

Riquelme, S., Schwarze, H., Fuentes, M., & Campos, J. Near Field Effects of Earthquake Rupture Velocity into Tsunami Run-up Heights. Journal of Geophysical Research: Solid Earth.

Okada, Y. (1985). Surface deformation due to shear and tensile faults in a half-space. Bulletin of the seismological society of America, 75(4), 1135-1154.

Satake, K., et al. (1993), Tsunami field survey of the 1992 Nicaragua earthquake, Eos Trans. AGU, 74(13), 145, 156–157, https://doi.org/10.1029/93EO00271

Satake, K. (1994). Mechanism of the 1992 Nicaragua tsunami earthquake. Geophysical Research Letters, 21(23), 2519-2522

Tanioka, Y., & Satake, K. (1996). Tsunami generation by horizontal displacement of ocean bottom. Geophysical Research Letters, 23(8), 861-864.

Titov, V., Song, Y. T., Tang, L., Bernard, E. N., Bar-Sever, Y., & Wei, Y. (2016). Consistent estimates of tsunami energy show promise for improved early warning. In Global Tsunami Science: Past and Future, Volume I (pp. 3863-3880). Birkhäuser, Cham.

Todorovska, M. I., & Trifunac, M. D. (2001). Generation of tsunamis by a slowly spreading uplift of the sea floor. Soil Dynamics and Earthquake Engineering, 21(2), 151-167.

Ward, S. N. (1980). Relationships of tsunami generation and an earthquake source. Journal of Physics of the Earth, 28(5), 441-474

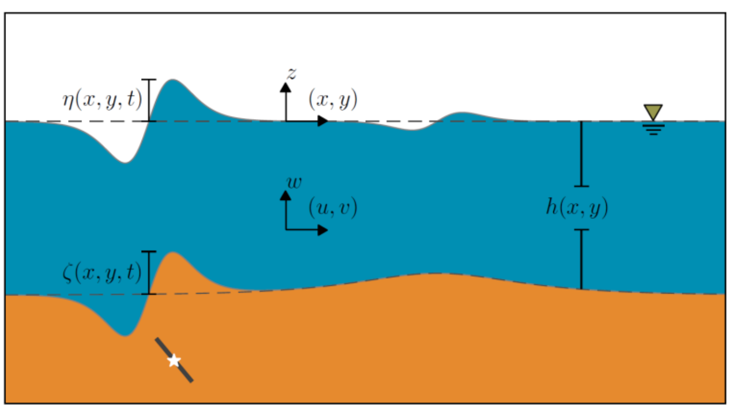

Figure 1. Tsunami variables for analytical modelation.

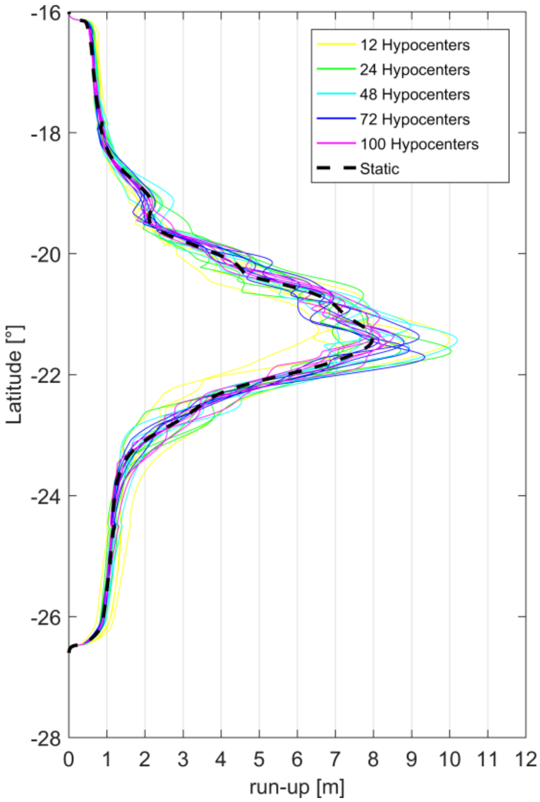

Figure 2. Run-up for heterogeneous scenarios earthquakes, with random (no causality) rupture starting points. While more random starting points the scenario tends to produce the same run-up that the static case scenario.

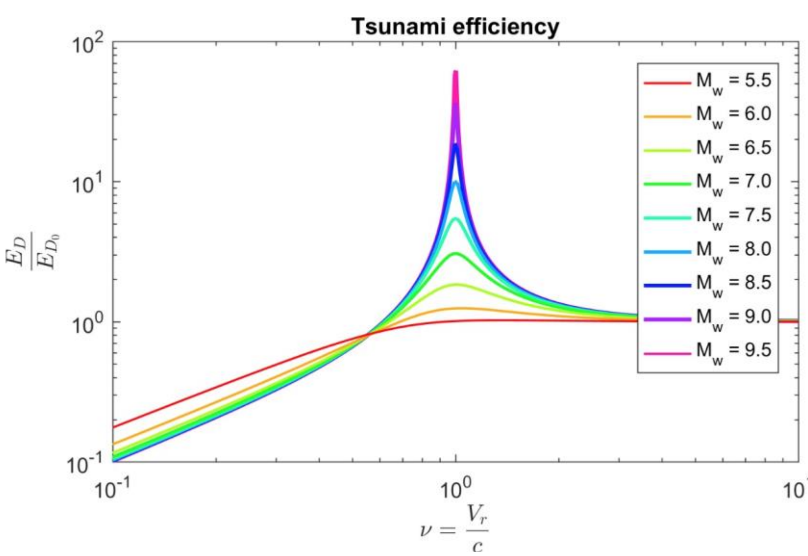

Figure 3. Tsunami Energy Efficiency $\frac{E_D}{E_{D_0}}$ as a function of V_r/c_0 . Large earthquakes tend to become larger when $V_r = c_0$. Small earthquakes do not amplify tsunami energy as much as large earthquakes.

Unilateral ED/ED0	**Rupture Velocity [km/s]**												**ED0**
Magnitude	**0.1**	**0.2**	**0.3**	**0.4**	**0.5**	**0.6**	**0.7**	**0.8**	**0.9**	**1.0**	**1.5**	**2.0**	**Infinite**
6	0.507	0.703	0.630	0.583	0.545	0.524	0.499	0.498	0.482	0.475	0.449	0.436	2.13E+10
6.5	0.401	1.069	0.912	0.808	0.732	0.680	0.654	0.629	0.622	0.611	0.574	0.559	2.59E+11
7	0.310	1.562	1.164	0.950	0.852	0.795	0.754	0.709	0.681	0.664	0.622	0.606	3.22E+12
7.5	0.267	2.158	1.218	1.015	0.933	0.858	0.811	0.762	0.746	0.723	0.649	0.643	3.41E+13
8	0.229	3.264	1.294	1.027	0.890	0.862	0.825	0.781	0.769	0.757	0.698	0.668	3.43E+14
8.5	0.209	5.183	1.463	1.045	0.917	0.873	0.856	0.807	0.793	0.783	0.711	0.690	3.44E+15
9	0.131	8.236	1.301	1.005	0.878	0.833	0.780	0.754	0.740	0.724	0.701	0.682	3.39E+16
9.5	0.205	9.333	1.144	0.841	0.841	0.756	0.716	0.687	0.695	0.743	0.662	0.662	3.30E+17

Table 1. Tsunami Efficiency for different earthquake moment magnitudes for an Unilateral Rupture.

Bilateral ED/ED0	**Rupture Velocity [km/s]**												**ED0**
Magnitude	**0.1**	**0.2**	**0.3**	**0.4**	**0.5**	**0.6**	**0.7**	**0.8**	**0.9**	**1.0**	**1.5**	**2.0**	Infinite
6	0.669	0.699	0.693	0.689	0.681	0.666	0.681	0.680	0.671	0.668	0.668	0.664	2.03E+10
6.5	0.782	0.935	0.859	0.823	0.815	0.792	0.782	0.786	0.784	0.779	0.770	0.763	2.58E+11
7	0.692	1.311	1.077	0.982	0.931	0.892	0.865	0.857	0.858	0.827	0.815	0.805	3.16E+12
7.5	0.505	1.988	1.350	1.136	1.047	0.971	0.942	0.920	0.913	0.899	0.864	0.844	3.37E+13
8	0.437	3.043	1.590	1.241	1.083	1.032	0.994	0.958	0.945	0.922	0.879	0.868	3.42E+14
8.5	0.431	3.851	1.562	1.165	1.069	1.006	0.935	0.902	0.885	0.879	0.846	0.840	3.44E+15
9	0.272	4.923	1.640	1.085	1.012	1.015	0.989	0.909	0.912	0.922	0.877	0.850	3.39E+16
9.5	0.006	9.209	1.436	0.991	0.882	0.837	0.813	0.788	0.792	0.774	0.776	0.785	3.30E+17

Table 2. Tsunami Efficiency for different earthquake moment magnitudes for a Bilateral Rupture.